J Mol Model (2014) 20:2514
DOI 10.1007/s00894-014-2514-z

ORIGINAL PAPER

Theoretical studies of palladium-catalyzed cycloaddition of alkynyl aryl ethers and alkynes

Qingxi Meng · Fen Wang

Received: 27 April 2014 / Accepted: 27 October 2014 / Published online: 18 November 2014

Abstract Density functional theory (DFT) was used to investigate palladium(0)-catalyzed cycloaddition of alkynyl aryl ethers and alkynes to generate 2-methylidene-2H-chromenes. Calculations indicated that the cycloaddition had five possible reaction pathways: I, II, III, IV, and V. In the palladium(0)-alkynyl aryl ether complex IM1, the oxidative addition of the C_{aryl}–H bond occurred prior to the dissociation of a ligand PMe_3. The dissociation of a ligand PMe_3 from the five-coordinated complex IM2 was much easier to achieve than the hydrogen transfer reaction and the substitution reaction of alkynes. In the palladium(0)-hydride complex IM4, the hydrogen migration of H1 from palladium to carbon C1 was much easier to achieve than migration to carbon C2. In the four-coordinated aryl-palladium-alkyne complexes IM6a and IM6b, the alkyne insertion reaction into the Pd–C_{aryl} bond occurred prior to that into the Pd–$C_{alkenyl}$ bond. The reaction channel IM1→TS1→IM2→IM4→TS3a→IM5a→IM6a→TS4a1→IM7a1→TS5a1→IM8a was the most favorable among the catalytic reaction pathways of the cycloaddition of alkynyl aryl ethers and 2-butynes catalyzed by the palladium(0)/PMe_3 complex. Moreover, hydrogen migration was the rate-determining step for this channel. The dominant product was 2-methylidene-2H-chromenes P1, which is in agreement with experimental studies.

Keywords Palladium-catalyzed cycloaddition · Alkynyl aryl ether · Alkyne · Reaction mechanism · Density functional theory

Introduction

Transition metal-catalyzed functionalization of C–H bonds is a rapidly growing field in synthetic organic chemistry and organometallic chemistry that enables efficient access to a wide variety of building blocks [1–5]. Much effort has naturally been devoted to developing more convenient and efficient strategies for catalytic C–H functionalization reactions. During the last three decades, many successful applications of catalytic C–H functionalization reactions directed toward the construction of C–C or C–N bonds have been reported in synthetic communities. Many transition metals, such as manganese [6], iron [7], cobalt [8], nickel [9], ruthenium [10], rhodium [11, 12], palladium [9, 13–17], iridium [18], and platinum [19] have been found to catalyze C–H functionalization reactions.

Recently, Minami et al. [13] reported palladium-catalyzed cycloaddition of alkynyl aryl ethers with alkynes via ortho C–H activation to give the product 2-methylidene-2H-chromenes in 93 % yield, as illustrated in Scheme 1. They showed that the active catalyst was the palladium(0) complex, and suggested a likely mechanism with two possible reaction pathways: C–H bond activation and cleavage, alkyne insertion, and reductive elimination; C–H bond activation, hydrogen migration, and alkyne insertion.

In order to understand the reaction mechanism of palladium(0)-catalyzed cycloaddition of alkynyl aryl ethers and alkynes to generate 2-methylidene-2H-chromenes, the cycloaddition of alkynyl aryl ethers and 2-butynes catalyzed by the palladium(0)/PMe_3 complex was studied in the present work. Specifically, this study focused on: (1) the energetics of the

Electronic supplementary material The online version of this article (doi:10.1007/s00894-014-2514-z) contains supplementary material, which is available to authorized users.

Q. Meng (✉)
College of Chemistry and Material Science, Shandong Agricultural University, Taian, Shandong 271018, People's Republic of China
e-mail: qingxim@sdau.edu.cn

F. Wang
Department of Chemistry, Taishan University, Taian, Shandong 271021, People's Republic of China

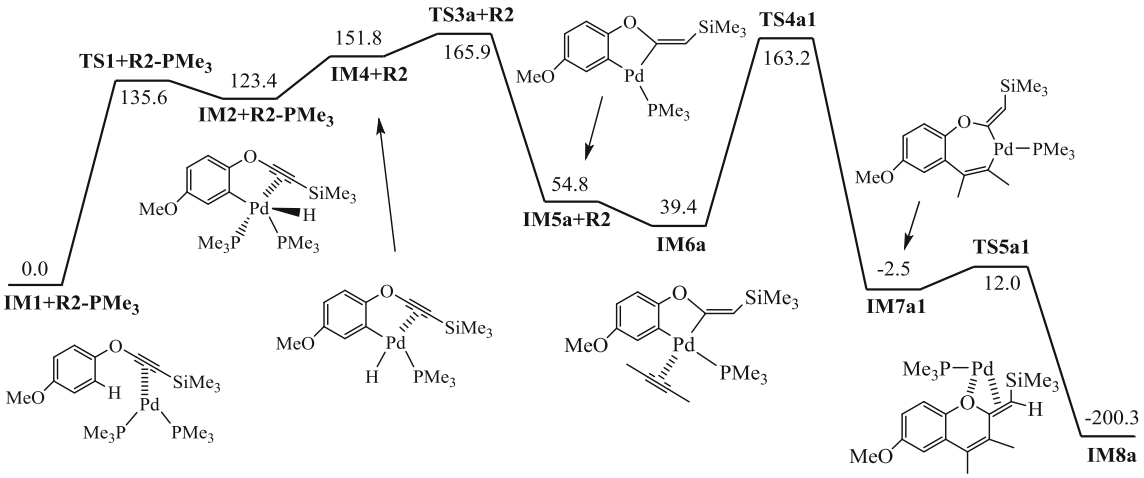

Fig. 1 Energy surface of the most favorable channel in the palladium-catalyzed cycloaddition of alkynyl aryl ethers with alkynes. Energies are in kJ mol^{-1}

overall catalytic reaction pathways in palladium(0)-catalyzed cycloaddition, (2) the structural features of intermediates and transition states, (3) the most favorable reaction channel, (4) the possible reaction channels of hydrogen migration, and (5) the possible pathways of alkyne insertion in this reaction mechanism. The possible reaction pathways of palladium(0)-catalyzed cycloaddition of alkynyl aryl ethers and 2-butynes are outlined in Scheme 2.

Computational details

All calculations were carried out with the Gaussian 09 programs [20]. The geometries of all the species were fully optimized using the density functional theory (DFT) [21] M06 method [22]. The 6-31G(d,p) basis set was used for carbon, oxygen, silicon, phosphorus, and hydrogen atoms, and the LANL2DZ basis set was used for palladium, adding one set of *f*-polarization function with an exponent of 1.472 [23]. Frequency calculations at the same computational level were performed to confirm each stationary point to be either a minimum (IM) or a transition structure (TS). The intermediates were characterized by all real frequencies. The TSs were verified by intrinsic reaction coordinate (IRC) [24] calculations and by animating the negative eigenvector coordinates with a visualization program (Molekel 4.3) [25, 26]. To obtain the starting structures for TS optimizations, the relaxed potential energy surface (PES) scan was performed to find an IRC of a maximum on the approximate elementary reaction channel. In addition, the bonding characteristics were analyzed by natural bond orbital (NBO) theory [27–30]. NBO analysis was performed by utilizing NBO5.0 code [31] at the same computational level. Furthermore, the electron densities, ρ, at the bond critical points (BCPs) or the ring critical points (RCPs) for some species were calculated with the AIM 2000 program package [32, 33].

Results and discussion

All the optimized structures in this reaction mechanism are illustrated in Figures S1–6 in the Supporting Information. The relative free energies ΔG, enthalpies ΔH, and ZPE corrected electronic energies ΔE are provided in Tables S1–2 in the Supporting Information. Unless otherwise noted, the discussed energies in the following are relative free energies ΔG.

C_{aryl}–H bond functionalization: oxidative addition of the C_{aryl}–H bond

As illustrated in Scheme 2, the oxidative addition of the C_{aryl}–H bond has two possible reaction pathways: the palladium(0)-alkynyl aryl ether complex IM1 went through the oxidative addition to give five-coordinated palladium(0)-hydride complex IM2 via a transition state TS1 with a free energy of

Scheme 1 Palladium-catalyzed cycloaddition of alkynyl aryl ethers with alkynes

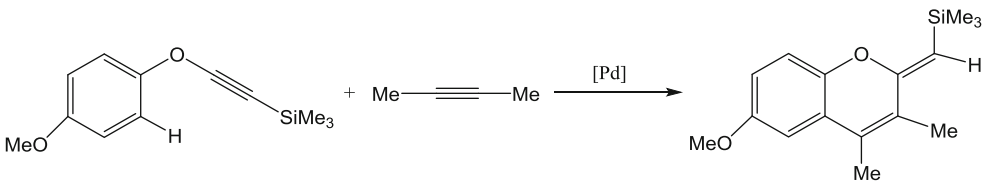

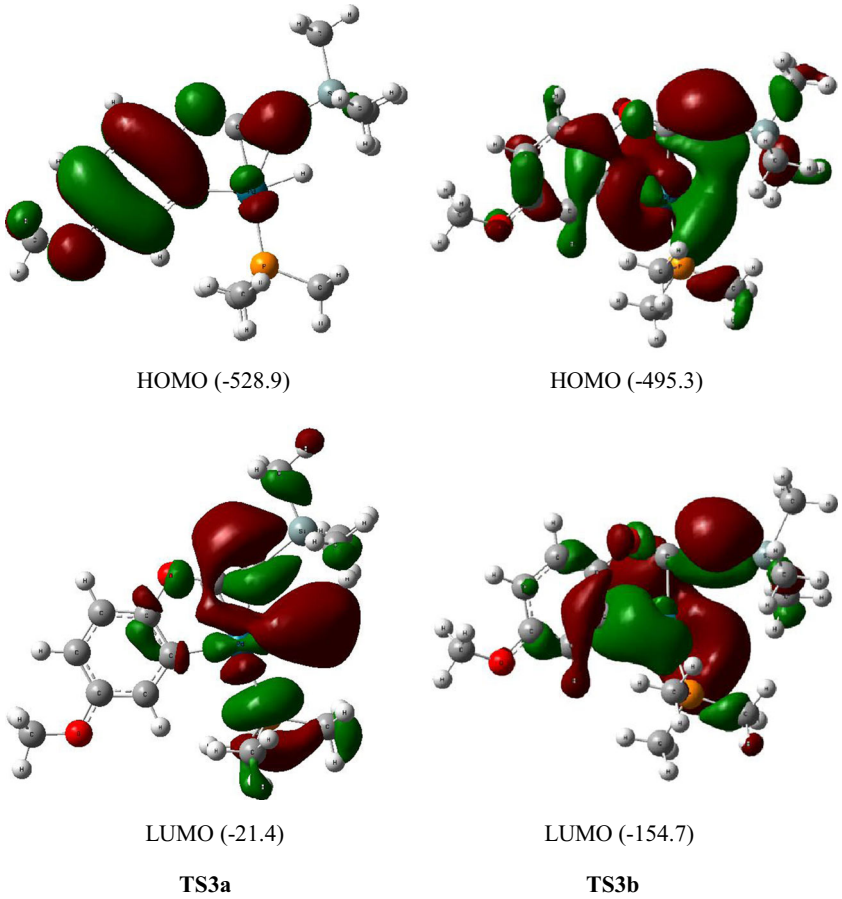

Fig. 2 Highest occupied molecular orbitals (HOMOs) and lowest unoccupied molecular orbitals (LUMOs) of TS3a and TS3b. Energies are in kJ mol^{-1}

135.6 kJ mol^{-1}, and then the dissociation of ligand PMe_3 from IM2 generated the active palladium(0)-hydride complex IM4; the dissociation of ligand PMe_3 from IM1 formed an active intermediate IM3, which would undergo the oxidative addition through TS2 with a free energy of 166.0 kJ mol^{-1}, leading to IM4. Hence, the first pathway was more dominant than the second.

NBO analysis of intermediate IM1 showed there was a back-donation π bond between palladium and the $\pi_{C1–C2}$ bond of alkynyl: the occupied π bonding orbital ($\pi_{C1–C2}$) acted on the empty hybridized orbital of palladium leading to a σ coordinate bond; on the other hand, the occupied d orbital (d_{xy}, d_{xz}, d_{yz}) of palladium acted on the empty π* antibonding orbital ($\pi^*_{C1–C2}$) leading to a π back-donation bond. In the oxidative addition of the C_{aryl}–H bond, the distance between C4 and H1, $d_{(C4–H1)}$, was 1.720, while $d_{(Pd–C4)}$ and $d_{(Pd–H1)}$ distances are 2.091, 1.608 Å, indicating significant interaction between Pd and H1, C4 occurred; conversely, the C4–H1 bond was weakened considerably, as demonstrated by analyzing the changes in bond orders P_{ij} and electron densities ρ at the BCPs (e.g., Pd–H1 bond, P_{ij}, IM1: 0.000→TS1: 0.299→IM2: 0.379; ρ, IM1: 0.000→TS1: 0.125→IM2: 0.134 e$Å^{-3}$). Transition state TS1 involved a Pd–C2–O1–C3–C4 five-membered ring, and the electron density of the RCP was 0.014 e $Å^{-3}$. The Pd-H1 and Pd-C4 bonds of IM2 were σ bond, and the orbital energies were −767.6 and −894.6 kJ mol^{-1}, respectively. NBO analysis of IM4 also showed the Pd-H1 and Pd-C4 bonds were σ bond, and the orbital energies were −829.8 and −922.6 kJ mol^{-1}, which were lower than those of IM2. The formation of the back-donation π bond between palladium and the $\pi_{C1–C2}$ bond of alkynyl in IM4 weakened and activated the C1–C2 bond, which would result in hydrogen migration.

The most favorable reaction channel: path I

Figure 1 shows the most favorable channel leading to 2-methylidene-2H-chromenes in the palladium(0)-catalyzed cycloaddition of alkynyl aryl ethers and 2-butynes. The hydrogen migration in IM4 had two possible reaction modes: the migration of H1 from Pd to C1 is denoted as "a", while that of H1 from Pd to C2 was denoted as "b". Intermediate IM4 went through a hydrogen transfer reaction via TS3a with a free energy of 165.9 kJ mol^{-1}, leading to complex IM5a. Next, the complexation of 2-butyne to IM5a generated complex IM6a. Intermediate IM6a then underwent the alkyne insertion reaction to form complex IM7a1, via the TS4a1 with a free energy of 163.2 kJ mol^{-1}. Finally, intermediate IM7a1

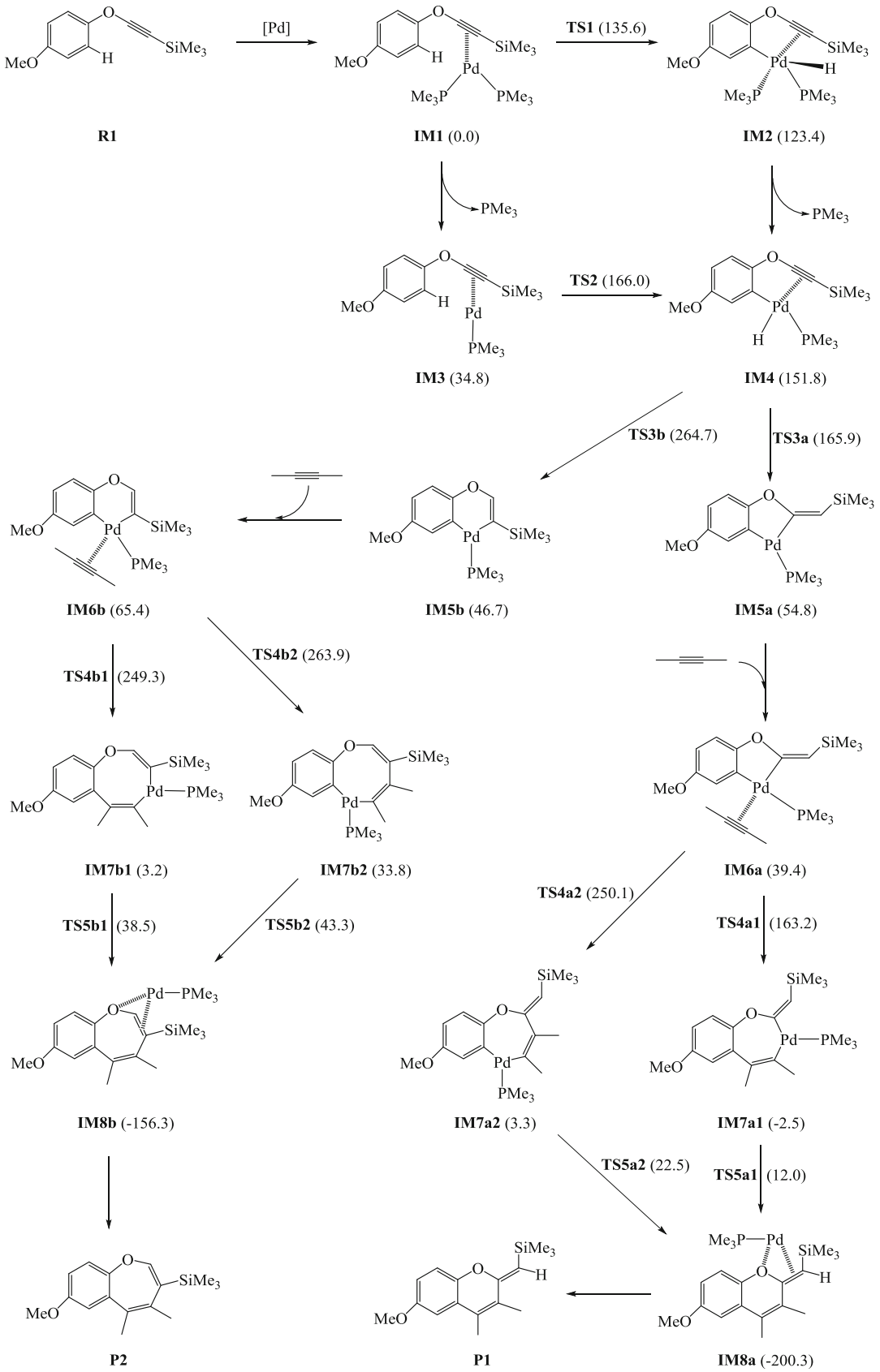

Scheme 2 Possible reaction mechanisms of palladium-catalyzed cycloaddition of alkynyl aryl ethers with alkynes (paths I and II). *Numbers in parentheses* are relative free energies ΔG in kJ mol^{-1}

underwent the reductive elimination reaction via TS TS5a1 with a free energy of 12.0 kJ mol^{-1} to generate the complex IM8a giving the product 2-methylidene-2H-chromene. Hence, hydrogen migration was the rate-determining step for this pathway.

The high stabilization energies of 157.4 and 206.8 kJ mol^{-1} for the $\pi_{C1-C2} \rightarrow \sigma^*_{Pd-H1}$ and $\pi_{C1-C2} \rightarrow (5s)_{Pd}$ in TS3a revealed the strong interaction between π_{C1-C2} and σ^*_{Pd-H1} and $(5s)_{Pd}$ orbital and the electron migration tendency from π_{C1-C2} to σ^*_{Pd-H1} and $(5s)_{Pd}$. NBO analysis of IM5a showed that both the Pd–C2 and Pd–C4 bonds were σ bonds, and their orbital energies were −985.5 and −977.1 kJ mol^{-1}, respectively. There was a back-donation π bond between palladium and the π_{C6-C7} bond in IM6a, and NBO analysis also showed that the Pd–C2 and Pd–C4 bonds were σ bonds, and the orbital energies were −993.2 and −945.9 kJ mol^{-1}. Relative to IM5a, the Pd–C4 bond was weakened and activated because of the formation of the back-donation π bond, which indicated that the alkyne insertion reaction was promoted. Therefore, the alkyne insertion reaction into the Pd–C4 bond occurred prior to that into the Pd–C2 bond. The high stabilization energies for the $\pi_{C6-C7} \rightarrow \sigma^*_{Pd-C4}$ and $(2p)_{C2} \rightarrow \sigma^*_{Pd-C4}$ in TS4a1 were 370.9 and 314.0 kJ mol^{-1}, which displayed the strong interaction between π_{C6-C7} or $(2p)_{C2}$ and σ^*_{Pd-C4} and the electron migration tendency from π_{C6-C7} or $(2p)_{C2}$ to σ^*_{Pd-C4}. The Pd–C2 and Pd–C7 bonds of IM7a1 showed the strong single-bond character.

The alkyne insertion in IM6a had two possible reaction modes: C6 attacking C4 was denoted as "a1", while C7 attacking C2 was denoted as "a2". Another reaction channel had also been studied: the free energies of the corresponding transition states TS4a2 and TS5a2 were 250.1 and 22.5 kJ mol^{-1}, which indicated that this channel was energetically prohibited. Therefore, in IM6a, the alkyne insertion reaction into the Pd–C_{aryl} bond occurred prior to that into the Pd–$C_{alkenyl}$ bond.

The reaction channels: path II

The reaction pathways (path II) are illustrated in Scheme 2: in IM4, the hydrogen migration of H1 from Pd to C2 is denoted as "b". The intermediates and transition states in these pathways were similar to those discussed above (path I). The free energies of the transition states TS3b, TS4b1, and TS5b1 were 264.7, 249.3, and 38.5 kJ mol^{-1}, respectively. Evidently, hydrogen migration was the rate-determining step for this pathway. Because the free energy of TS3b was higher than that of TS3a by 98.8 kJ mol^{-1}, the reaction pathways (path I) were more dominant than path II. As illustrated in Fig. 2, the HOMO of TS3a was lower than that of TS3b by 33.6 kJ mol^{-1}, while the LUMO of TS3a was higher than that of TS3b by 133.3 kJ mol^{-1}, so TS3a had better stability than TS3b, which agreed with those discussed above.

The other reaction channel was also studied: in IM6b, C6 attacking C4 was denoted as "b1", while C7 attacking C1 was denoted as "b2". The free energies of the transition states TS4b2 and TS5b2 were 263.9 and 43.3 kJ mol^{-1}, respectively, which indicated that this channel was also energetically prohibited. Hence, in IM6b, the alkyne insertion reaction into the Pd–C_{aryl} bond occurred prior to that into the Pd–$C_{alkenyl}$ bond, which is in agreement with those discussed above (path I).

The reaction channels: path III

As illustrated in Fig. 3, the intermediate IM2 underwent the hydrogen migration to deliver the complexes IM9a and IM9b via the corresponding transition states TS6a and TS6b. The

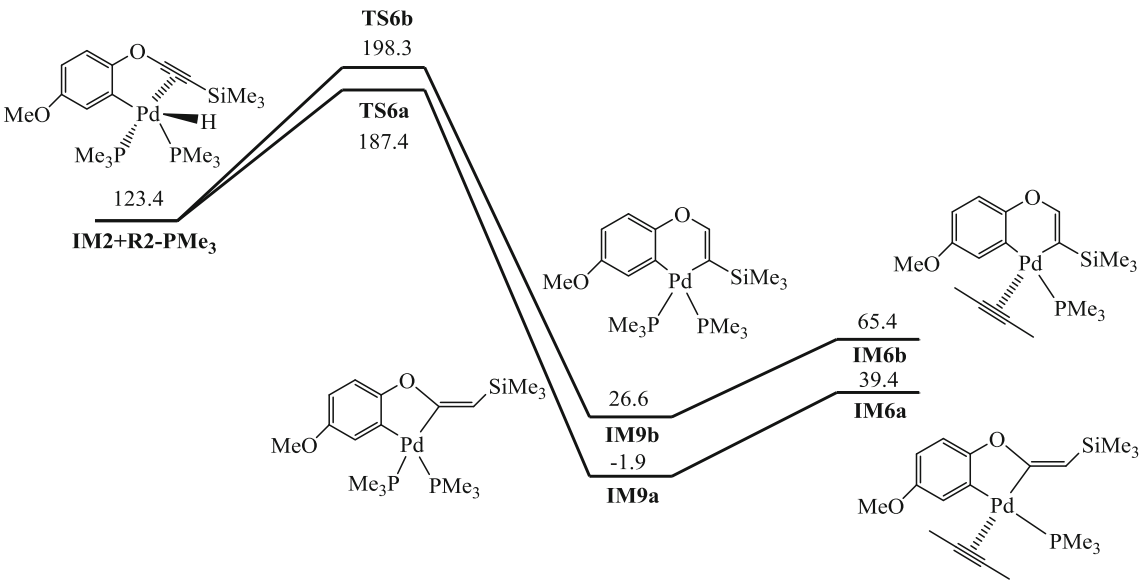

Fig. 3 Energy surface of palladium-catalyzed cycloaddition of alkynyl aryl ethers with alkynes (path III). Energies are in kJ mol^{-1}

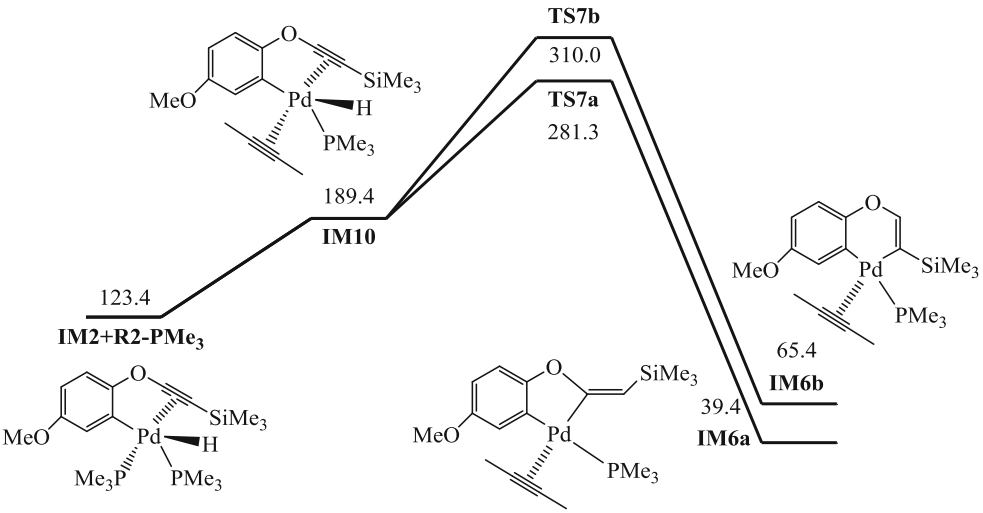

Fig. 4 Energy surface of palladium-catalyzed cycloaddition of alkynyl aryl ethers with alkynes (path IV). Energies are in kJ mol^{-1}

complexation of IM9a, IM9b and 2-butynes resulted in complexes IM6a, IM6b, respectively. The free energies of TS6a and TS6b were 187.4 and 198.3 kJ mol^{-1}, respectively, which were higher than TS3a by 21.5 and 32.4 kJ mol^{-1}, so reaction pathway path I was more dominant than path III. In the five-coordinated intermediate IM2, the dissociation of a ligand PMe_3 occurred prior to the hydrogen transfer reaction.

The reaction channels: path IV

Figure 4 shows the energy profiles of the reaction pathways (path IV). The intermediate IM2 coordinated to 2-butyne and formed a five-coordinated palladium-hydride complex IM10, and then IM10 went through hydrogen migration to complexes IM6a and IM6b via transition states TS7a and TS7b with free energies of 281.3 and 310.0 kJ mol^{-1}, respectively. The free energy of TS3a was much lower than those of TS7a and TS7b (by 115.4 and 144.1 kJ mol^{-1}, respectively) so the pathways (path IV) were energetically prohibited.

The reaction channels: path V

As illustrated in Fig. 5, the five-coordinated palladium-hydride complex IM10 underwent the alkyne insertion reaction through the transition state TS8 with a free energy of 278.9 kJ mol^{-1} to give complex IM11. Intermediate IM11 went through the cyclization reaction via the TS9a and TS9b with free energies of 122.5 and 115.4 kJ mol^{-1}, respectively, resulting in complexes IM12a and IM12b. Intermediates IM12a and IM12b underwent hydrogen migration to deliver complexes IM8a and IM8b, respectively, via transition states TS10a and TS10b with free energies of −5.8 and 0.9 kJ mol^{-1},

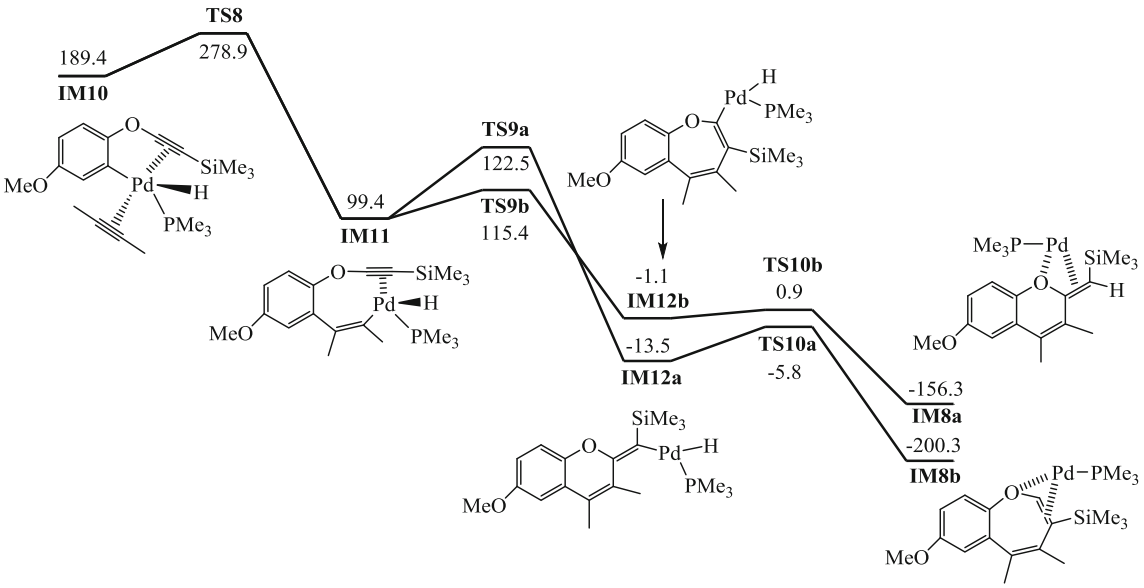

Fig. 5 Energy surface of palladium-catalyzed cycloaddition of alkynyl aryl ethers with alkynes (path V). Energies are in kJ mol^{-1}

respectively. Therefore, the alkyne insertion reaction was the rate-determining step for the pathway (path V), because the free energy of TS8 was the highest. The free energy of TS8 was much higher (by 113.0 kJ mol^{-1}) than that of TS3a, so the pathways (path V) were energetically prohibited.

Conclusions

The reaction mechanisms of palladium(0)-catalyzed cycloaddition of alkynyl aryl ethers and alkynes to give 2-methylidene-2H-chromenes were explored computationally using DFT methods [at M06/6-31G(d,p) level, LANL2DZ(f) for Pd]. The results indicated that the cycloaddition had five possible reaction pathways (I, II, III, IV, and V). In the palladium(0)-alkynyl aryl ether complex IM1, the oxidative addition of the C_{aryl}–H bond occurred prior to the dissociation of the ligand PMe_3. The dissociation of ligand PMe_3 from the five-coordinated complex IM2 was much easier to achieve than the hydrogen transfer reaction and the substitution reaction of alkynes. In the palladium(0)-hydride complex IM4, hydrogen migration of H1 from palladium to the carbon C1 was much easier to achieve than to carbon C2. In the four-coordinated aryl-palladium-alkyne complexes IM6a and IM6b, the alkyne insertion reaction into the Pd–C_{aryl} bond occurred prior to that into the Pd–$C_{alkenyl}$ bond.

The reaction channel IM1→TS1→IM2→IM4→TS3a→IM5a→IM6a→TS4a1→IM7a1→TS5a1→IM8a was the most favorable among all catalytic reaction pathways of the cycloaddition of alkynyl aryl ethers and 2-butynes catalyzed by the palladium(0)/PMe_3 complex. Hydrogen migration was the rate-determining step for this channel. The theoretically predicted dominant product was 2-methylidene-2H-chromenes P1, which was in well agreement with the experimental studies [13].

Acknowledgments This work was supported by the Natural Science Foundation of China (No. 31270723, 31370686), Technology Development Program of Shandong Province, China (No. 2013GZX20109), and Youth Science and Technology Innovation Foundation of Shandong Agricultural University (No. 23824).

Calculations reported in the paper were performed on the Gaussian 09 programs by the College of Chemistry and Chemical Engineering, Southwest University. The authors extend our heartfelt gratitude to the distinguished Professor Ming Li in Southwest University for current discussions.

References

1. Chen X, Engle KM, Wang DH, Yu JQ (2009) Palladium(II)-catalyzed C-H activation/C-C cross-coupling reactions: versatility and practicality. Angew Chem Int Ed 48:5094–5115
2. Johnson KRD, Hayes PG (2013) Cyclometalative C-H bond activation in rare earth and actinide metal complexes. Chem Soc Rev 42: 1947–1960
3. Musaev DG, Figg TM, Kaledin AL (2014) Versatile reactivity of Pd-catalysts: mechanistic features of the mono-*N*-protected amino acid ligand and cesium-halide base in Pd-catalyzed C-H bond functionalization. Chem Soc Rev 43:5009–5031. doi:10.1039/C3CS60447K
4. Baillie RA, Legzdins P (2014) Distinctive activation and functionalization of hydrocarbon C-H bonds initiated by $Cp^*W(NO)(\eta^3\text{-allyl})(CH_2CMe_3)$ complexes. Acc Chem Res 47: 330–340
5. Zhang XS, Chen K, Shi ZJ (2014) Transition metal-catalyzed direct nucleophilic addition of C–H bonds to carbon–heteroatom double bonds. Chem Sci 5:2146–2159. doi:10.1039/C3SC53115E
6. He R, Huang ZT, Zheng QY, Wang C (2014) Manganese-catalyzed dehydrogenative [4+2] annulation of N-H imines and alkynes by C-H/N-H activation. Angew Chem Int Ed. doi:10.1002/anie.201402575
7. Sirois JJ, Davis R, Deboef B (2014) Iron-catalyzed arylation of heterocycles via directed C-H bond activation. Org Lett 16:868–871
8. Semproni SP, Atienza CCH, Chirik PJ (2014) Oxidative addition and C–H activation chemistry with a PNP pincer-ligated cobalt complex. Chem Sci 5:1956–1960
9. Iaroshenko VO, Gevorgyan A, Davydova O, Villinger A, Langer P (2014) Regioselective and guided C-H activation of 4-nitropyrazoles. J Org Chem 79:2906–2915
10. Park Y, Jeon I, Shin S, Min J, Lee PH (2013) Ruthenium-catalyzed C-H activation/ cyclization for the synthesis of phosphaisocoumarins. J Org Chem 78:10209–10220
11. Huckins JR, Bercot EA, Thiel OR, Hwang TL, Bio MM (2013) Rh(III)-catalyzed C–H activation and double directing group strategy for the regioselective synthesis of naphthyridinones. J Am Chem Soc 135:14492–14495
12. Hu F, Xia Y, Ye F, Liu Z, Ma C, Zhang Y, Wang J (2014) Rhodium(III)-catalyzed *ortho* alkenylation of *N*-phenoxyacetamides with *N*-tosylhydrazones or diazoesters through C-H activation. Angew Chem Int Ed 53:1364–1367
13. Minami Y, Shiraishi Y, Yamada K, Hiyama T (2012) Palladium-catalyzed cycloaddition of alkynyl aryl ethers with internal alkynes via selective ortho C-H activation. J Am Chem Soc 134:6124–6127
14. Maleckis A, Kampf JW, Sanford MS (2013) A detailed study of acetate-assisted C-H activation at palladium(IV) centers. J Am Chem Soc 135:6618–6625
15. Takemoto S, Grushin VV (2013) Nucleophile-catalyzed, facile, and highly selective C–H activation of fluoroform with Pd(II). J Am Chem Soc 135:16837–16840
16. Zhang C, Ji J, Sun P (2014) Palladium-catalyzed alkenylation via sp^2 C–H bond activation using phenolic hydroxyl as the directing group. J Org Chem 79:3200–3205
17. Mahindra A, Bagra N, Jain R (2013) Palladium-catalyzed regioselective C-5 arylation of protected L-histidine: microwave-assisted C-H activation adjacent to donor arm. J Org Chem 78:10954–10959
18. Choi G, Tsurugi H, Mashima K (2013) Hemilabile N-xylyl-N'-methylperimidine carbene iridium complexes as catalysts for C-H activation and dehydrogenative silylation: dual role of N-xylyl moiety for ortho-C-H bond activation and reductive bond cleavage. J Am Chem Soc 135:13149–13161
19. Bowring MA, Bergman RG, Tilley TD (2013) Pt-catalyzed C–C activation induced by C-H activation. J Am Chem Soc 135:13121–13128
20. Frisch, MJ, Trucks GW, Schlegel HB, Scuseria GE, Robb MA, Cheeseman JR, Scalmani G, Barone V, Mennucci B, Petersson GA, Nakatsuji H, Caricato M, Li X, Hratchian HP, Izmaylov AF, Bloino J, Zheng G, Sonnenberg JL, Hada M, Ehara M, Toyota K, Fukuda R, Hasegawa J, Ishida M, Nakajima T, Honda Y, Kitao O, Nakai H,

Vreven T, Montgomery JAJr, Peralta JE, Ogliaro F, Bearpark M, Heyd JJ, Brothers E, Kudin KN, Staroverov VN, Kobayashi R, Normand J, Raghavachari K, Rendell A, Burant JC, Iyengar SS, Tomasi J, Cossi M, Rega N, Millam NJ, Klene M, Knox JE, Cross JB, Bakken V, Adamo C, Jaramillo J, Gomperts R, Stratmann RE, Yazyev O, Austin AJ, Cammi R, Pomelli C, Ochterski JW, Martin RL, Morokuma K, Zakrzewski VG, Voth GA, Salvador P, Dannenberg JJ, Dapprich S, Daniels AD, Farkas Ö, Foresman JB, Ortiz JV, Cioslowski J, Fox DJ (2009) Gaussian 09, Revision C.01, Gaussian, Inc., Wallingford CT

21. Parr RG, Yang W (1989) Density-functional theory of atoms and molecules. Oxford University Press, New York
22. Zhao Y, Truhlar DG (2008) The M06 suite of density functionals for main group thermochemistry, thermochemical kinetics, noncovalent interactions, excited states, and transition elements: two new functionals and systematic testing of four M06-class functionals and 12 other functionals. Theor Chem Accounts 120:215–241
23. Ehlers AW, Böhme M, Dapprich S, Gobbi A, Höllwarth A, Jonas V, Köhler KF, Stegmann R, Veldkamp A, Frenking G (1993) A set of f-polarization functions for pseudo-potential basis sets of the transition metals Sc–Cu, Y–Ag and La–Au. Chem Phys Lett 208:111–114
24. Gonzalez C, Schlegel HB (1990) Reaction path following in mass-weighted internal coordinates. J Phys Chem 94:5523–5527
25. Flükiger P, Lüthi HP, Portmann S, Weber J (2000–2002) MOLEKEL 4.3 Swiss Center for Scientific Computing, Manno. Switzerland
26. Portmann S, Lüthi HP (2000) An interactive molecular graphics tool. Chimia 54:766–770
27. Carpenter JE, Weinhold F (1988) Analysis of the geometry of the hydroxymethyl radical by the "different hybrids for different spins" natural bond orbital procedure. J Mol Struct (THEOCHEM) 169:41–50
28. Foster JP, Weinhold F (1980) Natural hybrid orbitals. J Am Chem Soc 102:7211–7218
29. Reed AE, Weinstock RB, Weinhold F (1985) Natural population analysis. J Chem Phys 83:735–746
30. Reed AE, Curtiss LA, Weinhold F (1988) Intermolecular interactions from a natural bond orbital, donor-acceptor viewpoint. Chem Rev 88: 899–926
31. Glendening ED, Badenhoop JK, Reed AE, Carpenter JE, Bohmann JA, Morales CM, Weinhold F (2001) NBO 5.0. Theoretical Chemistry Institute, University of Wisconsin, Madison
32. Bader RFW (1990) Atoms in molecules, a quantum theory; international series of monographs in chemistry, vol 22. Oxford University Press, Oxford
33. Biegler-König F, Schönbohm J, Derdau R, Bayles D, Bader RFW (2002) AIM 2000. Version 2.0, McMaster University.